

Rat brain pro-oxidant effects of peripherally administered 5 nm ceria 30 days after exposure

Sarita S. Hardas^a, Rukhsana Sultana^a, Govind Warriar^a, Mo Dan^b, Rebecca L. Florence^b, Peng Wu^c, Eric A. Grulke^c, Michael T. Tseng^d, Jason M. Unrine^e, Uschi M. Graham^f, Robert A. Yokel^{b,g}, D. Allan Butterfield^{a,h,*}

^a Department of Chemistry, University of Kentucky, Lexington, KY 40506-0055, United States

^b Department of Pharmaceutical Sciences, University of Kentucky Academic Medical Center, University of Kentucky, Lexington, KY 40536-0082, United States

^c Chemical and Materials Engineering Department, University of Kentucky, Lexington, KY 40506-0503, United States

^d Department of Anatomical Sciences & Neurobiology, University of Louisville, Louisville, KY 40202, United States

^e Department of Plant and Soil Sciences, University of Kentucky, Lexington, KY 40546-0091, United States

^f Center for Applied Energy Research, University of Kentucky, Lexington, KY 40511, United States

^g Graduate Center for Toxicology, University of Kentucky Academic Medical Center, Lexington, KY 40506-9983, United States

^h Center of Membrane Sciences, University of Kentucky, Lexington, KY 40506-0059, United States

ARTICLE INFO

Article history:

Received 21 January 2012

Accepted 15 June 2012

Available online 28 June 2012

Keywords:

Oxidative stress

Ceria

Brain

Neurotoxicity

Nanomaterial

Nanoparticles

Rat

ABSTRACT

The objective of this study was to determine the residual pro- or anti-oxidant effects in rat brain 30 days after systemic administration of a 5 nm citrate-stabilized ceria dispersion. A ~4% aqueous ceria dispersion was iv-infused (0 or 85 mg/kg) into rats which were terminated 30 days later. Ceria concentration, localization, and chemical speciation in the brain was assessed by inductively coupled plasma mass spectrometry (ICP-MS), light and electron microscopy (EM), and electron energy loss spectroscopy (EELS), respectively. Pro- or anti-oxidant effects were evaluated by measuring levels of protein carbonyls (PC), 3-nitrotyrosine (3NT), and protein-bound-4-hydroxy-2-trans-nonenal (HNE) in the hippocampus, cortex, and cerebellum. Glutathione reductase (GR), glutathione peroxidase (GPx), superoxide dismutase (SOD), and catalase levels and activity were measured in addition to levels of inducible nitric oxide (iNOS), and heat shock protein-70 (Hsp70). The blood brain barrier (BBB) was visibly intact and no ceria was seen in the brain cells. Ceria elevated PC and Hsp70 levels in hippocampus and cerebellum, while 3NT and iNOS levels were elevated in the cortex. Whereas glutathione peroxidase and catalase activity were decreased in the hippocampus, GR levels were decreased in the cortex, and GPx and catalase levels were decreased in the cerebellum. The GSH:GSSG ratio, an index of cellular redox status, was decreased in the hippocampus and cerebellum. The results are in accordance with the observation that this nanoscale material remains in this mammal model up to 30 days after its administration and the hypothesis that it exerts pro-oxidant effects on the brain without crossing the BBB. These results have important implications on the potential use of ceria ENM as therapeutic agents.

© 2012 Elsevier Inc. All rights reserved.

Abbreviations: 3NT, protein bound 3-nitrotyrosine; Ce, cerium; Cat, catalase; EELS, electron energy loss spectroscopy; ENM, engineered nanomaterial; GR, glutathione reductase; GPx, glutathione peroxidase; H₂O₂, hydrogen peroxide; Hsp70, heat shock protein 70; HNE, protein-bound 4-hydroxy-2-trans-nonenal; ICP-MS, inductively coupled plasma mass spectrometry; iNOS, inducible nitric oxide synthase; MDL, method detection limit; PC, protein carbonyl; ROS, reactive oxygen species; RNS, reactive nitrogen species; SOD, superoxide dismutase; TEM, transmission electron microscopy.

* Corresponding author at: Department of Chemistry, University of Kentucky, Lexington, KY 40506-0055, United States. Tel.: +1 859 257 3184; fax: +1 859 323 1069.

E-mail addresses: Sarita.Hardas@uky.edu (S.S. Hardas), rsult2@uky.edu (R. Sultana), govind.warrior@uky.edu (G. Warriar), mo.dan@uky.edu (M. Dan), rlstep2@uky.edu (R.L. Florence), peng.wu@uky.edu (P. Wu), eric.grulke@uky.edu (E.A. Grulke), mtttsen01@louisville.edu (M.T. Tseng), jason.unrine@uky.edu (J.M. Unrine), uschi.graham@uky.edu (U.M. Graham), ryokel@email.uky.edu (R.A. Yokel), dabcsn@uky.edu (D.A. Butterfield).

1. Introduction

Engineered nanomaterials (ENM) can be manufactured in a variety of shapes and sizes and physico-chemical, surface, as well as optical and magnetic properties. ENMs have numerous applications in research, medicine, electronics and other industries. Physico-chemical properties of nanomaterials differ from their bulk forms mainly because of the larger surface area to mass ratio, which affects reactivity, strength and electrical properties of nanomaterials. Because of their comparable size with biological molecules like proteins and DNA, ENMs can gain access to usually difficult to reach biological compartments in cells (Fubini et al., 2010). Increased surface activity can facilitate interactions with biological molecules, which may evoke greater physiological responses, different from the same basic material with larger particle size, the bulk form equivalent of ENMs (Donaldson et al., 2004; Landsiedel et al., 2009; Xia et al., 2009). One effect exhibited by ENMs is the generation of free radicals or induction of oxidative stress, which is also a primary mechanism of ENM toxicity (Xia et al., 2009). Oxidative stress effects are direct consequences of imbalance in the rates of reactive oxygen and/or nitrogen species (ROS or RNS) production versus scavenging of ROS and/or RNS and/or antioxidant levels (Butterfield et al., 2007).

Ceria ENM (a.k.a. cerium oxide; CeO₂), which is one of the most used ENM employed in different industrial applications (Yokel et al., 2009a,b; Hardas et al., 2010) has been shown to have both anti-inflammatory properties as well as potent toxicity. However, there is no clear understanding of what exactly controls ceria's pro- or anti-oxidant effects. A recently published report summarizes findings of *in vitro* and *in vivo* studies conducted with ceria ENM under basal and induced oxidative stress conditions (Celardo et al., 2011). Ceria exhibited antioxidant properties evidenced by scavenging free radicals, by reducing levels of peroxides, iNOS, TNF- α , NF- κ B, and interleukin, by promoting cell viability or protecting organelles from diesel exhaust and cigarette smoke-induced oxidative stress, ROS generating chemical agents, or side effects of radiation treatment. Ceria has been suggested for potential use in the treatment of diabetic cardiomyopathy, cancer, stroke, retinal degradation and Alzheimer's disease as well as to prolong life span (Chen et al., 2006; Rzigalinski et al., 2006; Das et al., 2007; Xia et al., 2008; D'Angelo et al., 2009; Hirst et al., 2009; Babu et al., 2010; Colon et al., 2010; Younce et al., 2010; Estevez et al., 2011; Niu et al., 2011). Antioxidant properties of ceria may be related to its SOD- and catalase-mimicking activity (Korsvik et al., 2007; Pirmohamed et al., 2010) attributed to Ce³⁺/Ce⁴⁺ redox coupling (Celardo et al., 2011). In contrast, there are reports of ceria induced pro-oxidant effects under basal conditions. In different cell culture studies, ceria ENM mediated ROS injury, induced lipid peroxidation, caused membrane damage, led to elevation of the cytokine, IL-8, led to depletion of GSH, and led to reduced cell viability (Brunner et al., 2006; Lin et al., 2006; Park et al., 2008; Auffan et al., 2009).

To utilize ceria for therapeutic and non-therapeutic applications, it is important to know the long term effects of intended and un-intended ceria exposure on mammals. Most reports on effects of ceria ENM were conducted using non-mammalian organisms or in cell culture, and none of these addressed long-term effects or fate of ceria. In addition to our own previous studies (Yokel et al., 2009a,b; Hardas et al., 2010), a few ceria ENM studies were conducted in intact animals (Chen et al., 2006; Niu et al., 2007; Hirst et al., 2009, 2011; Amin et al., 2011; Choi et al., 2011; Srinivas et al., 2011; Zhou et al., 2011). One study reports that deposition and retention of ceria in various vital organs and increased WBC count were seen 30 days after intraperitoneal and intravenous injection to mice, but otherwise ceria was tolerated by animals (Hirst et al., 2011). Ceria reduced myocardial oxidative stress in

transgenic mice for ischemic cardiomyopathy, rat liver from monocrotaline-induced ROS injury by induction of GSH levels and intravitreal injections of ceria inhibited retinal neovascular lesions (Niu et al., 2007; Amin et al., 2011; Zhou et al., 2011). However, after pulmonary inhalation of ceria ENM, granulomatous pathology and GSH depletion were seen in rat lungs (Cho et al., 2010; Srinivas et al., 2011). Animal studies have also reported that ceria ENM can accumulate in various organs, including the heart and lung, irrespective of the point of entry or distance (from injection point and organ specifically examined) when supplied as intravenous or intra-peritoneal injections or as a food additive (Chen et al., 2006; Niu et al., 2007; Hirst et al., 2009). This accumulation may lead to systemic effects involving the inflammatory response (Celardo et al., 2011) or increased ROS production under normal physiological conditions (Hirst et al., 2011).

To our knowledge there is no prior information available on the long-term effects (30 days or more after administration) of ceria on brain and how these effects may contrast with an immediate response after the initial ENM contact. Our previous study showed moderate pro-oxidant effects on rat brain, 1 and 20 h after a single acute systemic instillation of 5 nm ceria ENM (Hardas et al., 2010). The current study discusses residual effects of oxidative stress parameters in brain 30 days after one single acute ENM peripheral administration using 5 nm ceria ENM. To address the objective, the levels and activities of the antioxidant enzymes catalase, manganese superoxide dismutase (Mn-SOD), glutathione peroxidase (GPx), and glutathione reductase (GR), were measured along with the ratio of reduced glutathione (GSH) to its oxidized form (GSSG). To understand the extent of changes in cellular redox status, the levels of oxidative stress endpoints, protein carbonyl (PC), 3-nitrotyrosine (3NT), and protein bound 4-hydroxyl-2-trans nonenal (HNE), were measured along with heat shock protein (Hsp70) levels.

2. Materials and methods

All the materials, methods including the well characterized 5 nm ceria ENM are same as that used in our recently published study (Hardas et al., 2010). The rats used are of the same strain, sex and approximately same weight as that used in the previous study with 5 nm ceria ENM (Hardas et al., 2010). Therefore, only a brief overview is presented.

2.1. Nanomaterial

Cerium chloride heptahydrate (Sigma–Aldrich # 228931, 99.9% metal basis), ammonium hydroxide (Fisher #3256, ACS, 28–30%) and citric acid monohydrate (EMD Chemicals Inc. # CX1725-1, GR ACS) were used without further purification. A hydrothermal method was used to synthesize ~5 nm ceria aqueous suspension. Briefly, a 20 ml aqueous mixture of 0.01 mol cerium chloride and 0.01 M citric acid was added to 20 ml of 3 M ammonium hydroxide. After stirring for 24 h at 50 °C, the solution was transferred into a Teflon-lined stainless steel bomb and heated at 80 °C for 24 h to complete the reaction. The final dispersion of ceria ENM was infused intravenously to the rats over 1 h without any further treatment or purification.

2.2. Ceria characterization

The details of ceria ENM characterization are published in our earlier study (Hardas et al., 2010). In brief, the morphology and crystallinity of the ceria was evaluated using a 200-keV field emission analytical transmission electron microscope (JEOL JEM-2010F, Tokyo, Japan) equipped with an Oxford energy dispersive X-ray spectrometer. The particle size distributions (PSDs) were

determined using dynamic light scattering (DLS: Brookhaven Instruments Corporation, 90Plus NanoParticle Size Distribution Analyzer, Holtsville, NY, USA). The surface area of the dried ceria powder was determined using a BETASAP 2020 surface area analyzer that determines particle surface area based on nitrogen adsorption (Micromeritics Instrument Corporation, Norcross, GA, USA). The ceria content of the dispersion and the potential presence of contaminating elements/metals were determined by digestion of ceria dispersion samples and analysis by ICP-MS. Electron energy loss spectroscopy (EELS) was performed on rat liver tissue using a JEOL 2010F STEM outfitted with a URP pole piece, GATAN 2000 GIF (Pleasanton, CA, USA), GATAN DigiScan II, Fischione HAADF STEM detector (Export, PA, USA), and EmiSpec EsVision software (Tempe, AZ, USA).

2.3. Animals

In the current study 16 male Sprague Dawley rats, weighing 328 ± 21 g (mean \pm SD), were obtained from Harlan, Indianapolis, IN, and were housed individually prior to study and after cannulae removal (a few days after the iv infusion) in the University of Kentucky Division of Laboratory Animal Resources facility under a 12:12 h light:dark cycle at 70 ± 8 °F and 30–70% humidity. The rats had ad lib access to 2018 Harlan diet and RO water. All procedures involving animals were approved by the University of Kentucky Institutional Animal Care and Use Committee. The research was conducted in accordance with the Guiding Principles in the Use of Animals in Toxicology (<http://www.toxicology.org/ai/air/air6.asp>).

2.4. Ceria administration

Rats were prepared with 2 cannulae that terminated in the vena cava to administer the ceria dispersion or water (controls) in one and 1.8% sodium chloride in the second, to avoid agglomeration induced by sodium chloride or 10% sucrose, which are commonly added to prepare iso-osmotic solutions (Yokel et al., 2009a,b; Hardas et al., 2010). Seven rats received 0 and nine rats received 85 mg ceria/kg as a single acute dose of ENM. The rats were terminated 30 days after the infusion. Post-mortem samples including brain cortex, hippocampus, and cerebellum were harvested rapidly and were frozen in liquid nitrogen and stored at -80 °C for later oxidative stress measurements. Cerium concentrations in brain cortex, blood, and liver were analyzed by ICP-MS; Agilent 7500cx (Santa Clara, CA, USA) after microwave digestion as described previously (Hardas et al., 2010). The detection limits of this method were 0.089 mg Ce/kg. Mean spike recovery ranged from 97 to 105%. Relative percent difference between replicates was $\leq 2\%$ for 30–120 ng Ce/ml and 18% for 1.5 ng Ce/ml.

2.5. Light and electron microscopic assessment

After animal termination brains were removed, sliced coronally in a brain matrix (Braintree acrylic matrix BS-A 6000C). Sections containing hippocampus were fixed by immersion in 4% buffered formalin. Cerebellum was similarly sliced and fixed. Samples were cut into 3 mm cubes, dehydrated and embedded in Araldite 502. After polymerization, one micron thick sections were cut and stained with toluidine blue for LM examination. Selected blocks were sectioned at 80 nm, collected on 200 mesh copper grids and examined in a Philips CM 10 electron microscope at 60 kV.

2.6. Oxidative stress assessment, sample preparation

All sample preparation and protein assays were carried out as described in our previous publication (Hardas et al., 2010). Each

sample was individually thawed and homogenized using a 550 sonic dismembrator from Fischer Scientific for 10–20 s on ice. The buffer used for homogenization contained 0.32 M sucrose, 0.125 M Tris, 0.6 mM $MgCl_2$, and protease inhibitors (4 μ g/ul leupeptin, 4 μ g/ul pepstatin A, 5 μ g/ul aprotinin, and 0.2 mM phenylmethylsulfonyl fluoride) at pH 8.0. Total protein concentration for each sample was measured using the bicinchoninic acid assay and equal amounts of protein from control and treated samples were used in each assay.

2.7. Oxidative stress markers

The oxidative stress markers PC, 3NT, and HNE were assessed for each homogenized sample using the slot blot technique. Specific antibodies were used to determine the levels of PC, 3NT, HNE in controls and treated samples as previously described (Hardas et al., 2010).

2.8. GSH and GSSG levels

The reduced (GSH) and oxidized glutathione (GSSG) levels were simultaneously measured in each sample as previously described (Hissin and Hilf, 1976). A small amount of brain tissue was rapidly weighed, homogenized with metaphosphoric acid (25%) and sodium phosphate (0.1 M) – ethylenediaminetetraacetic acid (0.005 M) buffer (pH 8) and then centrifuged. For GSH levels, an aliquot of supernatant was further diluted with phosphate buffer and then incubated with o-phthaldehyde (OPT), before determination of fluorescence (λ excitation 350 nm and emission 420 nm). For GSSG levels equal volumes of supernatant were incubated with N-ethylmaleimide (0.04 M) for 30 min and then diluted with sodium hydroxide (0.1 N), before assaying with OPT. The GSH to GSSG ratio for each sample was calculated by comparing the fluorescence values from each assay to their respective calibration curves. The final values are % control of mean \pm SEM of treated vs. control samples.

2.9. Western blot analysis

The levels of the antioxidant enzymes GR, GPx, MnSOD, catalase, Hsp70 and iNOS were measured using immunoblotting-Western blot techniques as described in our earlier publications (Sultana et al., 2008; Hardas et al., 2010). In brief, 75 μ g protein from each homogenized sample was loaded and separated on SDS-PAGE alongside its respective control. The separated proteins were transferred from poly-acrylamide gels to nitrocellulose membranes, and then the band of specific protein identified using a specific antibody against that protein. The band-intensity was quantified as previously described (Hardas et al., 2010) by using the image analysis software, ImageQuant, purchased from GE Healthcare.

2.10. Enzyme activity assays

The activities of GR, GPx, MnSOD and catalase enzymes were measured as described earlier (Hardas et al., 2010), with commercially available kits from Cayman Chemical Company, Ann Arbor, MI, USA as per the manufacturer's instructions. Suitable protein samples from each organ (i.e., 10–20 μ g for brain homogenate) were mixed with assay buffer and with other specific reagents for each assay on 96-well plates. Enzymatic reactions were initiated by addition of reaction initiator reagents, NADPH for GR, cumene hydroperoxide for GPx, xanthine oxidase for SOD, and hydrogen peroxide for the catalase assay. Progression of the each reaction was studied separately by spectrophotometry at 340 nm (for GR and GPx), at 460 nm (for SOD) and at 540 nm (for catalase).

2.11. Data and statistical analysis

The slot blot, Western blot and enzyme assay results are presented as mean \pm SEM. The control mean was normalized to 100%. Grubb's test was used to identify outliers in oxidative stress parameter results. Student's unpaired *t*-test was used to evaluate significant difference between controls and ceria treated samples. Subsequently, two-way ANOVA was conducted to determine the differential effect of ceria ENM treatment among the three brain regions studied. Significance was accepted at $p < 0.05$.

3. Results

3.1. Ceria composition

HR-TEM/HR-STEM showed the ceria ENM was polyhedral shaped (Fig. 1). The XRD patterns demonstrated the ceria was highly crystalline, with face centered cubic unit cells with corresponding Miller indices of the most common faces of (1 1 1), (2 1 0) and (2 0 0). Evaluation of a number of TEM images showed that the ceria had a number-average primary particle size of ~ 5 nm. The ceria ENM surface area was $121 \text{ m}^2/\text{g}$, assuming the density of a ceria nanoparticle $7600 \text{ kg}/\text{m}^3$ (the bulk density), the back-calculated average diameter should be 6.5 nm that fits our TEM observation quite well. Analysis by ICP-MS of the ceria dispersion used showed that the ceria content of the as-synthesized dispersion was $4.35 \pm 0.20\%$ and the free cerium ion content was $11.6 \pm 0.3\%$.

3.2. Dispersion properties

The citrate ion was found to be a stabilizing electrolyte for ceria nanoparticles. At pH below 7.0 the ceria agglomerated; therefore, the ceria was maintained as an aqueous dispersion at pH 7.7–8. Zeta potential of the citrate-stabilized particles was $-53 \pm 7 \text{ mV}$ at pH ~ 7.35 (Hardas et al., 2010). In general, dispersions with absolute values of zeta potential greater than 30–40 mV are expected to be stable, and the stability of dispersion is better with higher zeta potential. The cerium concentration in samples taken from the top and bottom of two ceria dispersion samples in covered 15 ml centrifuge tubes that were un-disturbed for >2 months were within 2.5% of each other, demonstrating dispersion stability (data not shown).

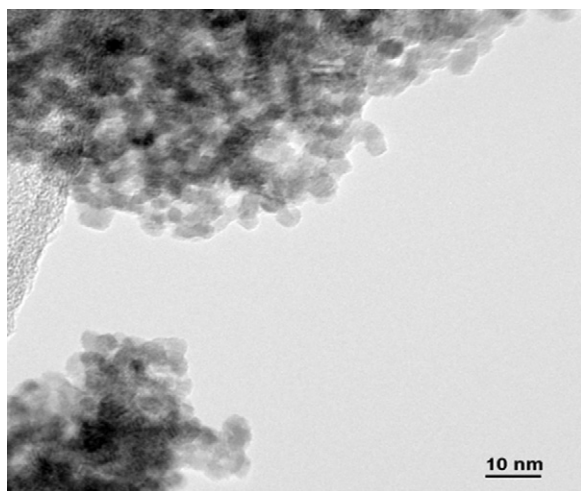


Fig. 1. Ceria ENM imaged using HRTEM. The ceria were dispersed on a carbon film. Visually they have a narrow size distribution ranging from 4 to 6 nm, the majority 5 nm.

3.3. Ceria concentration in brain and electron micrography

ICP-MS analysis showed that a very small amount of ceria was present in the brain compared to the liver (Table 1). Electron micrographic studies suggested that ceria ENM was not present in the brain, but located on the luminal side of the blood brain barrier (BBB) endothelium. The hippocampus and cerebellum tissues did not show obvious ceria induced injury as no necrotic neurons or elevated gliosis were observed and the BBB was visibly intact (data not shown).

3.4. EELS results

Electron energy loss spectroscopic (EELS) measurements on liver tissue were performed as a representative organ. The 5 nm ceria agglomerates were located in the tissue 30 days after infusion into rats. The ratio of Ce(3+) to Ce(4+) was evaluated using EELS measurements in vivo 30 days post infusion. Further, this ratio was compared with the ratio of $\text{Ce}^{3+}/\text{Ce}^{4+}$ obtained in freshly synthesized ceria. The high $\text{Ce}^{3+}/\text{Ce}^{4+}$ ratio that was obtained in the as-synthesized, fresh 5 nm ceria particles seems to have only been altered slightly in individual ceria measured in liver after 30 days in vivo. However, this difference was not significant (data not shown).

3.5. Oxidative stress indices

The primary aim of these studies was to evaluate indices of oxidative stress in brain 30 days following a single ceria ENM administration.

3.6. Ceria treatment affected catalase levels and activities

Previously ceria ENM was reported to have a H_2O_2 -producing ability (Korsvik et al., 2007); therefore, the effect of 5 nm ceria ENM on levels and activity of a primary H_2O_2 -reducing enzyme (catalase) was determined in the present study. Catalase activity was significantly decreased in the hippocampus ($\sim 18\%$, $*p < 0.05$, Fig. 2b) and catalase levels were significantly decreased in the cerebellum ($\sim 16\%$, $*p < 0.05$, Fig. 4a). To determine the influence of ceria treatment on the SOD enzyme or contribution to H_2O_2 levels from SODs, if any, the level of MnSOD and its activity were measured. There were no significant changes observed in the levels or activity of MnSOD (data not shown).

3.7. Ceria treatment decreases GPx levels, activity and the GSH-GSSG ratio

GPx reduces H_2O_2 along with other peroxides using glutathione (GSH) as a source of reducing equivalents. The activity of GPx was significantly decreased in the hippocampus ($\sim 69\%$, $**p < 0.001$, Fig. 2b) and in cerebellum ($\sim 23\%$, $*p < 0.05$, Fig. 4b). GPx levels showed a decreasing trend in all brain regions, but was significantly decreased only in cerebellum ($\sim 27\%$, $*p < 0.05$,

Table 1

Cerium concentrations in blood, brain, and liver, expressed as concentration and as a percentage of the ceria ENM dose. [Ce] in mg/kg wet weight of the blood or tissue (mean \pm SD).

	Cerium concentration [Ce] (mg/kg) wet weight and as a % of the ceria ENM dose ^a		
	Blood (mg/kg)	Brain (mg/kg)	Liver (mg/kg)
[Ce]	0.11 ± 0.16	0.38 ± 0.52	505 ± 238
% Dose	0.01 ± 0.02	0.008 ± 0.009	44 ± 27

^a Based on reference volume of blood in the rat (7% of body weight) or weight of the brain or liver times the ceria concentration.

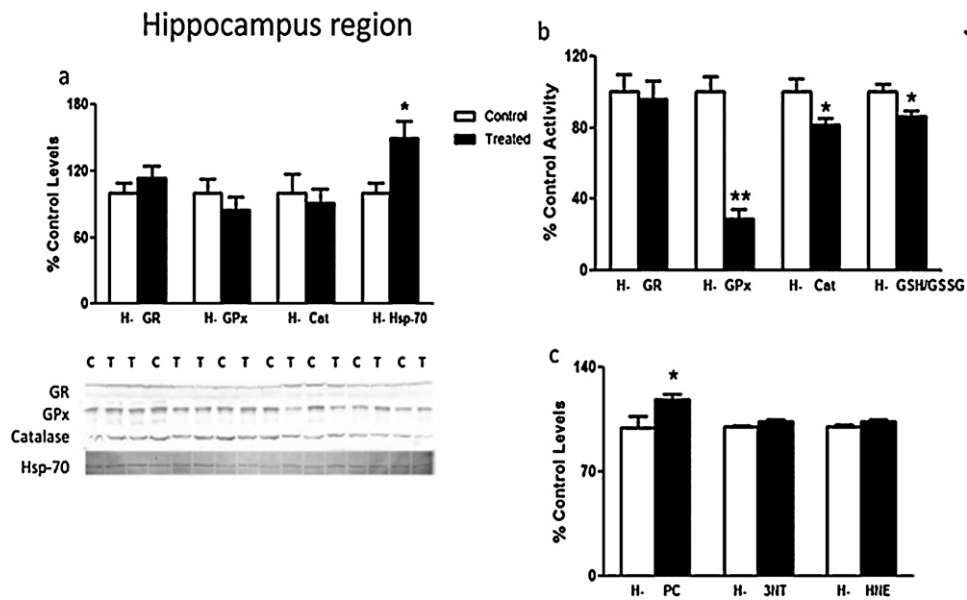


Fig. 2. In hippocampus 30 days after a single acute dose of 5 nm ceria ENM: (a) histograms showing GR, GPx, catalase, antioxidant enzymes and Hsp70 heat shock protein levels and corresponding Western blot experiments showing protein levels in control [C] and treated [T] samples. The intensity of each band was normalized with intensity of corresponding band of β -actin-loading control (not shown); (b) GR, GPx catalase antioxidant activities, and GSH:GSSG ratio measured in control and ceria treated samples; and (c) oxidative stress markers PC, 3NT and HNE levels. The values are calculated as % control for each measurement expressed as mean \pm SEM, control $n = 7$, treated $n = 9$, * $p < 0.05$, ** $p < 0.01$, compared to control.

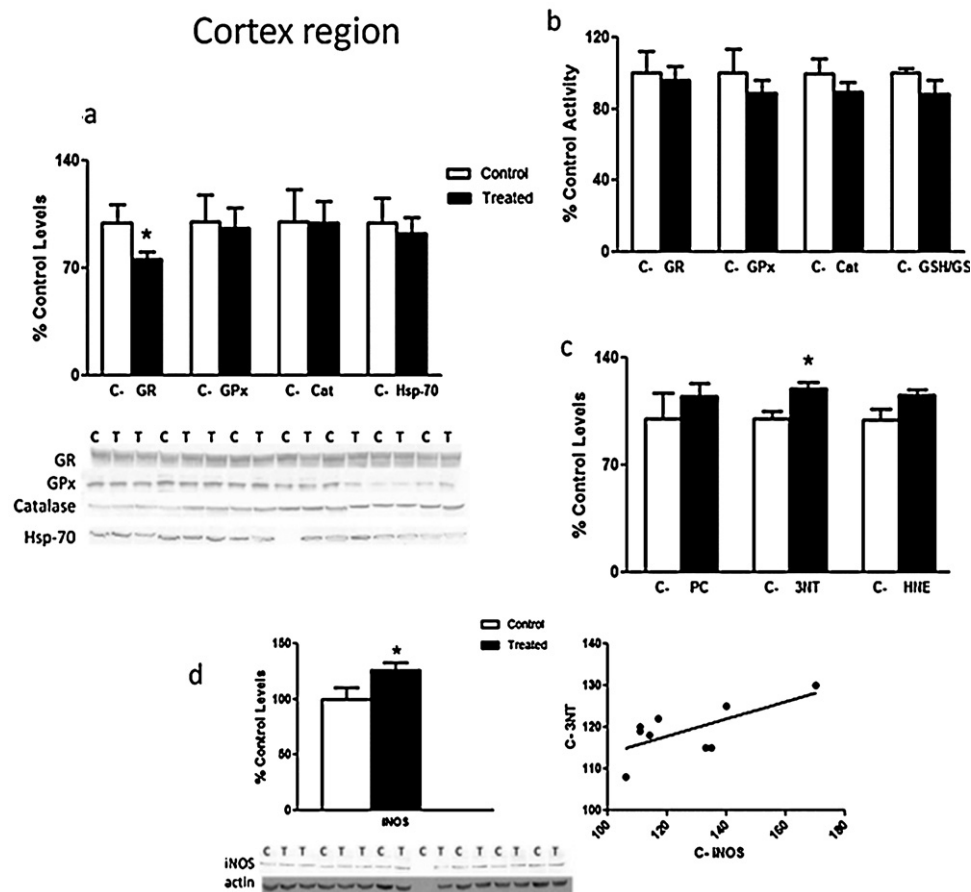


Fig. 3. In cortex 30 days after a single acute dose of 5 nm ceria ENM: (a) histograms showing GR, GPx, catalase, antioxidant enzymes and Hsp70 heat shock protein levels and corresponding Western blot experiments showing protein levels in control [C] and treated [T] samples. The intensity of each band was normalized with intensity of corresponding band of β -actin-loading control (not shown); (b) GR, GPx, catalase, antioxidants activities and GSH:GSSG ratio measured in control and ceria treated samples; (c) oxidative stress markers PC, 3NT and HNE levels, and (d) iNOS levels and correlation between 3NT levels and iNOS levels in ceria treated samples, $n = 9$, $r = 0.67$, $p < 0.05$. The values are calculated as % control for each measurement expressed as mean \pm SEM, control $n = 7$, treated $n = 9$, * $p < 0.05$, ** $p < 0.01$, compared to control.

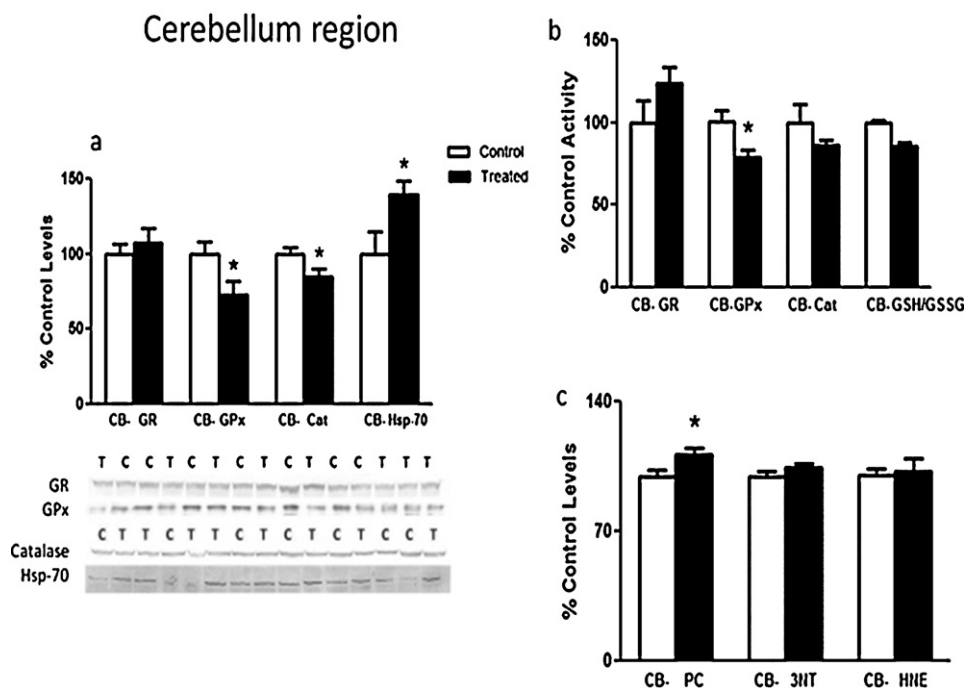


Fig. 4. In cerebellum 30 days after a single acute dose of 5 nm ceria ENM: (a) histograms showing GR, GPx, catalase, antioxidant enzymes and Hsp70 heat shock protein levels and corresponding Western blot experiments showing protein levels in control [C] and treated [T] samples. The intensity of each band was normalized with intensity of corresponding band of β -actin-loading control (not shown); (b) GR, GPx, catalase, antioxidants activities, and GSH:GSSG ratio measured in control and ceria treated samples, and (c) oxidative stress markers PC, 3NT and HNE levels. The values are calculated as % control for each measurement expressed as mean \pm SEM, control $n = 7$, treated $n = 8$, * $p < 0.05$, ** $p < 0.01$, compared to control.

Fig. 4a). Within the three brain regions examined, hippocampal GPx activity was significantly inhibited compared to that in cortex and cerebellum (** $p < 0.01$). GR levels were significantly decreased ($\sim 24\%$, * $p < 0.05$, Fig. 3a) in the cortex. GR activity did not show any significant change in any of the three brain regions studied. A marker of overall cellular redox status was evaluated by comparing the GSH:GSSG ratio of ceria-treated samples. The GSH:GSSG ratio was significantly decreased in the hippocampus ($\sim 13\%$, * $p < 0.05$, Fig. 2b) and cerebellum ($\sim 15\%$, ** $p < 0.01$, Fig. 4b) consistent with an increase in oxidative stress.

3.8. Ceria treatment induced protein oxidation

The levels of PC showed a significant increase in the hippocampus ($\sim 19\%$, * $p < 0.05$, Fig. 2c) and cerebellum ($\sim 12\%$, * $p < 0.05$, Fig. 4c) in treated vs. control samples. 3NT levels were significantly increased in the cortex ($\sim 20\%$, * $p < 0.05$, Fig. 3c). There was no significant change in protein-bound HNE levels in any of the three brain regions examined. Consistent with increased 3NT levels in cortical region, iNOS levels were increased significantly ($\sim 27\%$, * $p < 0.05$, Fig. 3d), and there was a positive correlation between 3NT and iNOS levels ($r = 0.67$, $p < 0.05$, Fig. 3d).

3.9. Hsp-70 levels increased after ceria treatment

Hsp-70 is a member of the heat shock protein family and inducible by oxidative stress. Hsp-70 levels were significantly increased in the hippocampus ($\sim 49\%$, * $p < 0.05$, Fig. 2a), as well as compared to that of cortical and cerebellar Hsp70 levels (* $p < 0.05$). In the cerebellum Hsp70 levels were increased ($\sim 40\%$, * $p < 0.05$, Fig. 4a). These results are consistent with diminution of GSH levels indicated by the decreased GSH:GSSG ratio in these brain regions.

4. Discussion

The present work was conducted to evaluate the oxidative stress effects of ceria ENM in brain 30 days after a single acute peripheral administration of 5 nm ceria ENM. ROS and RNS are inevitable byproducts of all major metabolic cellular processes and conspicuous by their high reactivity and high cytotoxicity. Apart from being a cause for many pathological conditions or cellular disturbances, ROS/RNS also play important roles in cell signaling pathways and cellular homeostasis (Celardo et al., 2011; Butterfield et al., 2001). Therefore, balancing excessive and insufficient ROS/RNS is critical, and endogenous enzymes like GPx, GR, catalase and SOD as well as antioxidants like glutathione maintain this redox balance efficiently. Any perturbation to this redox balance causes oxidative stress. One of the mechanisms by which nanomaterials induce toxicity is by inducing ROS production, elevating oxidative stress, which damages proteins, lipids or DNA (Butterfield and Stadtman, 1997; Nel et al., 2006; Sharma and Sharma, 2007; Mocan et al., 2010).

Owing to its redox switching between two oxidation states, 3+ and 4+, ceria exhibits catalytic activity, which has made it useful in industrial applications (Celardo et al., 2011). Ceria's surface redox capability can affect the immediate surroundings and has been strongly linked to particle size (Gilliss et al., 2005). The characteristic oxidation and reduction in ceria ENM is linked to the continued possibility to absorb and release oxygen by inducing oxygen vacancies close to the particle surface. The $\text{Ce}^{3+}/\text{Ce}^{4+}$ valance switch resembles redox behavior of some biological antioxidant enzymes like SOD and catalase. The high $\text{Ce}^{3+}/\text{Ce}^{4+}$ ratio is responsible for the ceria ENM SOD-mimetic activity (Korsvik et al., 2007).

In our previous study, the same 5 nm ceria ENM at the same dose as used in the present study showed moderate effects, on brain redox status, while catalase levels and activities were

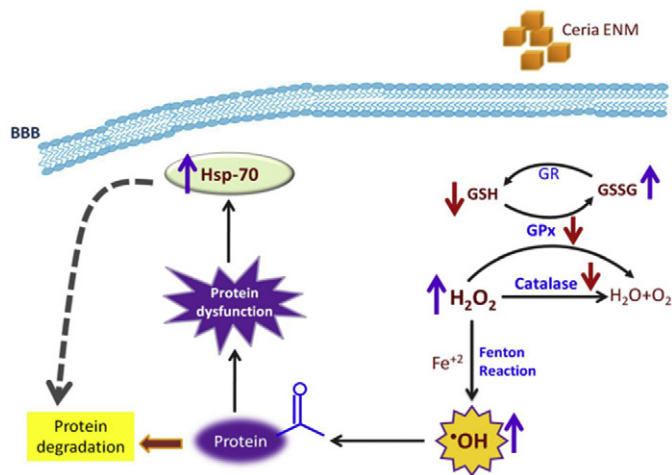


Fig. 5. In this proposed pathway ceria ENM induces pro-oxidant effects on rat brain without crossing BBB. Ceria ENM indirectly induces ROS production leading to GSH depletion and inhibition of catalase and GPx enzymes. This inhibition of H_2O_2 reducing enzyme activity can induce H_2O_2 levels and therefore hydroxyl radicals (OH^\bullet) production mediated by Fenton reaction. Increased OH^\bullet can further oxidize the proteins and may hamper their regular function. Hydroxyl radicals may also inhibit H_2O_2 reducing catalase and GPx activity by way of oxidative modification. These biochemical reactions could make cellular environment more oxidizing, triggering a cellular stress response to induce Hsp-70 levels. Hsp-70 is a chaperone protein that can shepherd oxidized proteins to the 20S proteasome for degradation for further cellular clearance (shown as dotted arrow). If timely clearance of oxidized protein takes place then there may not be any change in cellular PC levels. As there was no evidence of the presence of ceria ENM inside the brain, it is further proposed that ceria ENM exert their pro-oxidant effect in the brain secondary to its peripheral effects.

increased in hippocampus after 1 and 20 h, respectively, and catalase activity was decreased in cerebellum after 1 h. No change was seen in PC, 3NT and HNE levels (Hardas et al., 2010). Although, ceria ENM was not found in the brain, but located on the luminal side of the BBB endothelial cells and the BBB was intact, the current study demonstrated that 5 nm ceria ENM produced significant pro-oxidant effects in the brain 30 days following administration and their retention in peripheral organs (Fig. 5). Based on the EELS analysis, it would appear that even after a long-term exposure time of 30 days ceria continued to show a significant +3 valence on the surface. Similar high +3 valence was observed on surface of ceria ENM after short-term retention inside the rat, as seen in our previous study (Hardas et al., 2010), which was not significantly different compared to freshly prepared ceria. This finding clearly defines an enhanced oxygen storage capacity (Nesic et al., 2004) of the ceria surfaces that does not diminish greatly throughout the 30 day exposure period. Yet, ceria with enhanced OSC was shown in the current study to have a significant pro-oxidative effect in the brain after the long-term exposure following a single administration.

As depicted in Fig. 5, a decline in the GSH:GSSG ratio (in hippocampus and cerebellum) in the current study indicates elevated oxidative stress in the cellular environment. A similar observation was reported in Park et al. in which 30 nm ceria depleted GSH levels in human lung epithelial cells in a dose-dependent manner (Park et al., 2008). Hydroxylated derivatives of fullerenes also decreased the GSH:GSSG ratio and induced lipid peroxidation (Nakagawa et al., 2011). At the cellular level the GSH:GSSG ratio is dependent on GPx and GR enzymes, and in the current study we observed decreased GPx activity (in hippocampus and cerebellum), decreased GPx levels (in cerebellum) and decreased GR levels (cortex). Similarly, 15 nm silver and 90 nm copper ENM down-regulated GPx gene expression (Wang et al., 2009), 25 nm silver ENM (Rahman et al., 2009) and SWCNT (Wang et al., 2011) inhibited GPx activity, and silica ENM reduced GR

activity (Akhtar et al., 2010). Thus it may be possible that after 30 days following administration, ENM have deleterious effects on enzymes needed for maintenance of the reduced thiol status of the cells (Fig. 5).

Fig. 5 also shows that inhibition of catalase and GPx activities may lead to accumulation of H_2O_2 and ultimately increased production of hydroxyl radicals (OH^\bullet). Activity of catalase can be inhibited by hydroxyl radicals (OH^\bullet) and that of GPx by H_2O_2 and hydroperoxides (Pigeolet et al., 1990). Ceria ENM can produce H_2O_2 under abiotic conditions (Korsvik et al., 2007; Xia et al., 2008), and H_2O_2 has high membrane permeability (Halliwell, 1992). Further H_2O_2 can undergo a Fenton-type reaction to produce highly potent OH^\bullet radicals as noted above (Fig. 5). A lack of change in SOD activity and level in the current study may imply that endogenous SOD does not account for ceria-induced elevated oxidative stress in brain. Therefore, ceria ENM treatment may have caused induction in ROS that led to oxidative inhibition of antioxidant enzyme activities, decreased the GSH:GSSG ratio and increased in PC and 3NT levels observed in the present study. Similar consequences of oxidative stress were seen after exposure to various other ENM, such as TiO_2 (Hao et al., 2009; Liang et al., 2009; Xiong et al., 2011), SWCNT (Wang et al., 2011), MWCNT (Guo et al., 2011), hematite (Radu et al., 2010), and ZnO (Xia et al., 2008).

The elevated 3NT levels, a marker for increased nitrosive stress, are consistent with elevated levels of inducible nitric oxide synthase (iNOS). iNOS exists at extremely low levels under normal physiological conditions, but it is inducible by endotoxin and inflammatory cytokines among other stresses (Calabrese et al., 2000). We found a correlation between 3NT levels and iNOS levels in the cortical region of rats examined 30 days after ceria ENM treatment. It may indicate that increased 3NT levels are due to increased NO production in the cortex and we speculate that iNOS levels concurrently may be induced following ceria treatment via increased cytokine production.

Electron micrograph analysis showed an intact BBB and an absence of any significant amount of ceria in the brain. However, cobalt–chromium ENMs have damaged DNAs without crossing cellular membranes (Bhabra et al., 2009), and the chemotherapeutic drug doxorubicin led to neurotoxic effects without ever crossing the BBB (Tangpong et al., 2006). Similarly, it is conceivable that the observed oxidative stress response in brain regions could be due to the accumulation of 5 nm ceria in peripheral organs and subsequent elevation of BBB-permeable inflammatory cytokines. Studies to test this notion are in progress.

Induction of heat shock protein Hsp-70 levels as seen in the present study is in agreement with other literature reports. Similar to effects of silver ENM (Ahamed et al., 2010) and fullerene C60 (Usenko et al., 2008) treatments, Hsp-70 levels and other oxidative stress markers were induced with concomitant decrease in the GSH:GSSG ratio. In a transgenic mouse model for cardiomyopathy, Hsp-70 levels were increased as an oxidative stress marker of ER stress. Ceria ENM treatment rescued these cells from ER stress and as a result Hsp-70 expression was down regulated (Niu et al., 2007). In the present study, 5 nm ceria ENM indirectly induced ROS production in brain causing depletion of GSH, which initially induces antioxidant levels but over 30 days eventually inhibits H_2O_2 -scavenging catalase and GPx enzyme activities. This may increase H_2O_2 levels and therefore OH^\bullet production via the Fenton reaction, which may cause protein oxidation and induction of Hsp 70 levels (Fig. 5).

The pro-oxidant effects observed in the brain 30 days after a single intravenous administration of 5 nm ceria ENM are similar to those observed in age-related or Alzheimer disease-related oxidative stress effects previously reported by our laboratory (Butterfield et al., 2001; Butterfield and Stadtman, 1997). Although all three brain regions showed an effect of 5 nm ceria ENM

treatment, the extent of changes in oxidative stress indices was not same for all three brain regions. Therefore, depending upon which brain region is affected, the function of that brain region will be compromised. The EELS data suggests that mechanisms other than the valence switching between Ce⁴⁺ and Ce³⁺ oxidation states and the possibility to absorb and release oxygen by inducing oxygen vacancies must play a critically important role in pro-oxidant effects of ceria ENM. At present it is difficult to speculate why 5 nm ceria ENM did not cross the BBB. However, oxidative stress effects induced in brain may have been caused by some peripheral inflammatory cytokines that cross the BBB or by ROS generated as a result of long-term accumulation of 5 nm ceria ENM in peripheral organs.

5. Conclusions

Although short term time exposure to ceria in vivo leads to a relatively small initial biochemical response (Hardas et al., 2010), ceria administration may prove to be more harmful in the long term. As reported here a single acute dose of 5 nm ceria ENM can adversely affect brain redox status after 30 days. The important point to be noted is that, ceria may induce pro-oxidant effects without crossing or disturbing BBB. The elevated oxidative stress in particular brain regions may compromise brain functions and conceivably could even lead to neurodegeneration. Thus, implications of our study are profound for the proposed use of ceria ENM in therapeutic/non-therapeutic applications, which may lead to human exposure. Therefore, caution is suggested until and unless such effects as we demonstrated here can be mitigated.

Conflict of interest

None declared.

Acknowledgements

This work was supported by United States Environmental Protection Agency Science to Achieve Results [grant number RD-833772]. Although the research described in this article has been funded wholly or in part by the United States Environmental Protection Agency through STAR Grant RD-833772, it has not been subjected to the Agency's required peer and policy review and therefore does not necessarily reflect the views of the Agency and no official endorsement should be inferred.

References

Ahamed M, Posgai R, Gorey TJ, Nielsen M, Hussain SM, Rowe JJ. Silver nanoparticles induced heat shock protein 70, oxidative stress and apoptosis in *Drosophila melanogaster*. *Toxicol Appl Pharmacol* 2010;242(3):263–9.

Akhtar MJ, Ahamed M, Kumar S, Siddiqui H, Patil G, Ashquin M, et al. Nanotoxicity of pure silica mediated through oxidant generation rather than glutathione depletion in human lung epithelial cells. *Toxicology* 2010;276(2):95–102.

Amin KA, Hassan MS, Awad el-ST, Hashem KS. The protective effects of cerium oxide nanoparticles against hepatic oxidative damage induced by monocrotaline. *Int J Nanomed* 2011;6:143–9.

Auffan M, Rose J, Orsiere T, De Meo M, Thill A, Zeyons O, et al. CeO₂ nanoparticles induce DNA damage towards human dermal fibroblasts in vitro. *Nanotoxicology* 2009;3(2):161–71.

Babu S, Cho J-H, Dowding JM, Heckert E, Komanski C, Das S, et al. Multicolored redox active upconverter cerium oxide nanoparticle for bio-imaging and therapeutics. *Chem Commun* 2010;46(37):6915–7.

Bhabra G, Sood A, Fisher B, Cartwright L, Saunders M, Evans WH, et al. Nanoparticles can cause DNA damage across a cellular barrier. *Nat Nanotechnol* 2009;4(12):876–83.

Brunner TJ, Wick P, Manser P, Spohn P, Grass RN, Limbach LK, et al. In vitro cytotoxicity of oxide nanoparticles: comparison to asbestos, silica, and the effect of particle solubility. *Environ Sci Technol* 2006;40(14):4374–81.

Butterfield DA, Drake J, Pocernich C, Castegna A. Evidence of oxidative damage in Alzheimer's disease brain: Central role of amyloid β -peptide. *Trends Mol Med* 2001;7:548–54.

Butterfield DA, Stadtman ER. Protein oxidation processes in aging brain. *Adv Cell Aging Gerontol* 1997;2:161–91.

Butterfield DA, Reed T, Newman SF, Sultana R. Roles of amyloid [beta]-peptide-associated oxidative stress and brain protein modifications in the pathogenesis of Alzheimer's disease and mild cognitive impairment. *Free Radic Biol Med* 2007;43(5):658–77.

Calabrese V, Bates TE, Stella AMG. NO synthase and NO-dependent signal pathways in brain aging and neurodegenerative disorders: the role of oxidant/antioxidant balance. *Neurochem Res* 2000;25(9–10):1315–41.

Celardo I, Pedersen JZ, Traversa E, Ghibelli L. Pharmacological potential of cerium oxide nanoparticles. *Nanoscale* 2011;3(4):1411–20.

Chen JP, Patil S, Seal S, McGinnis JF. Rare earth nanoparticles prevent retinal degeneration induced by intracellular peroxides. *Nat Nanotechnol* 2006;1(2):142–50.

Cho W-S, Duffin R, Poland CA, Howie SEM, MacNee W, Bradley M, et al. Metal oxide nanoparticles induce unique inflammatory footprints in the lung: important implications for nanoparticle testing. *Environ Health Perspect* 2010;118(12):1699–706.

Choi J, Reipa V, Hitchins VM, Goering PL, Malinauskas RA. Physicochemical characterization and in vitro hemolysis evaluation of silver nanoparticles. *Toxicol Sci* 2011;123(1):133–43.

Colon J, Hsieh N, Ferguson A, Kupelian P, Seal S, Jenkins DW, et al. Cerium oxide nanoparticles protect gastrointestinal epithelium from radiation-induced damage by reduction of reactive oxygen species and upregulation of superoxide dismutase 2. *Nanomed Nanotechnol Biol Med* 2010;6(5):698–705.

D'Angelo B, Santucci S, Benedetti E, Di Loreto S, Phani RA, Falone S, et al. Cerium oxide nanoparticles trigger neuronal survival in a human Alzheimer disease model by modulating BDNF pathway. *Curr Nanosci* 2009;5(2):167–76.

Das M, Patil S, Bhargava N, Kang JF, Riedel LM, Seal S, et al. Auto-catalytic ceria nanoparticles offer neuroprotection to adult rat spinal cord neurons. *Biomaterials* 2007;28(10):1918–25.

Donaldson K, Stone V, Tran CL, Kreyling W, Borm PJA. Nanotoxicology. *Occup Environ Med* 2004;61(9):727–8.

Estevez AY, Pritchard S, Harper K, Aston JW, Lynch A, Lucky JJ, et al. Neuroprotective mechanisms of cerium oxide nanoparticles in a mouse hippocampal brain slice model of ischemia. *Free Radic Biol Med* 2011;51(6):1155–63.

Fubini B, Ghiazza M, Fenoglio I. Physico-chemical features of engineered nanoparticles relevant to their toxicity. *Nanotoxicology* 2010;4(4):347–63.

Gilliss SR, Bentley J, Carter CB. Electron energy-loss spectroscopic study of the surface of ceria abrasives. *Appl Surf Sci* 2005;241(1–2):61–7.

Guo Y-Y, Zhang J, Zheng Y-F, Yang J, Zhu X-Q. Cytotoxic and genotoxic effects of multi-wall carbon nanotubes on human umbilical vein endothelial cells in vitro. *Mutat Res Genet Toxicol Environ Mutagen* 2011;721(2):184–91.

Halliwell B. Reactive oxygen species and the central-nervous-system. *J Neurochem* 1992;59(5):1609–23.

Hao L, Wang Z, Xing B. Effect of sub-acute exposure to TiO₂ nanoparticles on oxidative stress and histopathological changes in Juvenile Carp (*Cyprinus carpio*). *J Environ Sci* 2009;21(10):1459–66.

Hardas SS, Butterfield DA, Sultana R, Tseng MT, Dan M, Florence RL, et al. Brain distribution and toxicological evaluation of a systemically delivered engineered nanoscale ceria. *Toxicol Sci* 2010;116(2):562–76.

Hirst SM, Karakoti A, Singh S, Self W, Tyler R, Seal S, et al. Bio-distribution and in vivo antioxidant effects of cerium oxide nanoparticles in mice. *Environ Toxicol* 2011. <http://dx.doi.org/10.1002/tox.20704>.

Hirst SM, Karakoti AS, Tyler RD, Sriranganathan N, Seal S, Reilly CM. Anti-inflammatory properties of cerium oxide nanoparticles. *Small* 2009;5(24):2848–56.

Hissin PJ, Hilf R. A fluorometric method for determination of oxidized and reduced glutathione in tissues. *Anal Biochem* 1976;74(1):214–26.

Korsvik C, Patil S, Seal S, Self WT. Superoxide dismutase mimetic properties exhibited by vacancy engineered ceria nanoparticles. *Chem Commun* (10):2007;1056–8.

Landsiedel R, Kapp MD, Schulz M, Wiench K, Oesch F. Genotoxicity investigations on nanomaterials: methods, preparation and characterization of test material, potential artifacts and limitations—many questions, some answers. *Mutat Res Rev Mutat Res* 2009;681(2–3):241–58.

Liang G, Pu Y, Yin L, Liu R, Ye B, Su Y, et al. Influence of different sizes of titanium dioxide nanoparticles on hepatic and renal functions in rats with correlation to oxidative stress. *J Toxicol Environ Health A* 2009;72(11–12):740–5.

Lin WS, Huang YW, Zhou XD, Ma YF. Toxicity of cerium oxide nanoparticles in human lung cancer cells. *Int J Toxicol* 2006;25(6):451–7.

Mocan T, Clichici S, Agoșton-Coldea L, Mocan L, Simon S, Ilie IR, et al. Implications of oxidative stress mechanisms in toxicity of nanoparticles (review). *Acta Physiol Hung* 2010;97(3):247–55.

Nakagawa Y, Suzuki T, Ishii H, Nakae D, Ogata A. Cytotoxic effects of hydroxylated fullerenes on isolated rat hepatocytes via mitochondrial dysfunction. *Arch Toxicol* 2011;85(11):1429–40.

Nel A, Xia T, Madler L, Li N. Toxic potential of materials at the nanolevel. *Science* 2006;311(5761):622–7.

Nesic O, Xu G-Y, McAdoo D, Westlund High K, Hulsebosch C, Perez-Polo R. IL-1 receptor antagonist prevents apoptosis and caspase-3 activation after spinal cord injury. *J Neurotrauma* 2004;18(9):947–56.

Niu J, Azfer A, Rogers LM, Wang X, Kolattukudy PE. Cardioprotective effects of cerium oxide nanoparticles in a transgenic murine model of cardiomyopathy. *Cardiovasc Res* 2007;73(3):549–59.

Niu J, Wang K, Kolattukudy PE. Cerium oxide nanoparticles inhibits oxidative stress and nuclear factor- κ B activation in H9c2 cardiomyocytes exposed to cigarette smoke extract. *J Pharmacol Exp Ther* 2011;338(1):53–61.

Park EJ, Choi J, Park YK, Park K. Oxidative stress induced by cerium oxide nanoparticles in cultured BEAS-2B cells. *Toxicology* 2008;245(1–2):90–100.

Pigeolet E, Corbisier P, Houbion A, Lambert D, Michiels C, Raes M, et al. Glutathione-peroxidase, superoxide-dismutase, and catalase inactivation by peroxides and oxygen derived free-radicals. *Mech Ageing Dev* 1990;51(3):283–97.

- Pirmohamed T, Dowding JM, Singh S, Wasserman B, Heckert E, Karakoti AS, et al. Nanoceria exhibit redox state-dependent catalase mimetic activity. *Chem Commun* 2010;46(16):2736–8.
- Radu M, Munteanu MC, Petrache S, Serban AR, Dinu D, Hermenean A, et al. Depletion of intracellular glutathione and increased lipid peroxidation mediate cytotoxicity of hematite nanoparticles in MRC-5 cells. *Acta Biochim Pol* 2010;57(3):355–60.
- Rahman MF, Wang J, Patterson TA, Saini UT, Robinson BL, Newport GD, et al. Expression of genes related to oxidative stress in the mouse brain after exposure to silver-25 nanoparticles. *Toxicol Lett* 2009;187(1):15–21.
- Rzagalinski BA, Meehan K, Davis RM, Xu Y, Miles WC, Cohen CA. Radical nanomedicine. *Nanomedicine (Lond)* 2006;1(4):399–412.
- Sharma HS, Sharma A. Nanoparticles aggravate heat stress induced cognitive deficits, blood–brain barrier disruption, edema formation and brain pathology. *Progress in brain research*, vol. 162. Elsevier; 2007 p. 245–73.
- Srinivas A, Rao PJ, Selvam G, Murthy PB, Reddy PN. Acute inhalation toxicity of cerium oxide nanoparticles in rats. *Toxicol Lett* 2011;205(2):105–15.
- Sultana R, Piroddi M, Galli F, Butterfield DA. Protein levels and activity of some antioxidant enzymes in hippocampus of subjects with amnesic mild cognitive impairment. *Neurochem Res* 2008;33(12):2540–6.
- Tangpong J, Cole MP, Sultana R, Joshi G, Estus S, Vore M, et al. Adriamycin-induced, TNF- α -mediated central nervous system toxicity. *Neurobiol Dis* 2006;23(1):127–39.
- Usenko CY, Harper SL, Tanguay RL. Fullerene C60 exposure elicits an oxidative stress response in embryonic zebrafish. *Toxicol Appl Pharmacol* 2008;229(1):44–55.
- Wang J, Rahman MF, Duhart HM, Newport GD, Patterson TA, Murdock RC, et al. Expression changes of dopaminergic system-related genes in PC12 cells induced by manganese, silver, or copper nanoparticles. *Neurotoxicology* 2009;30(6):926–33.
- Wang J, Sun P, Bao Y, Liu J, An L. Cytotoxicity of single-walled carbon nanotubes on PC12 cells. *Toxicol In Vitro* 2011;25(1):242–50.
- Xia T, Kovochich M, Liang M, Madler L, Gilbert B, Shi H, et al. Comparison of the mechanism of toxicity of zinc oxide and cerium oxide nanoparticles based on dissolution and oxidative stress properties. *ACS Nano* 2008;2(10):2121–34.
- Xia T, Li N, Nel AE. Potential health impact of nanoparticles. *Annu Rev Public Health* 2009;30(1):137–50.
- Xiong D, Fang T, Yu L, Sima X, Zhu W. Effects of nano-scale TiO₂, ZnO and their bulk counterparts on zebrafish: acute toxicity, oxidative stress and oxidative damage. *Sci Total Environ* 2011;409(8):1444–52.
- Yokel RA, Florence RL, Unrine JM, Tseng MT, Graham UM, Wu P, et al. Biodistribution and oxidative stress effects of a systemically-introduced commercial ceria engineered nanomaterial. *Nanotoxicology* 2009a;3(3):234–48.
- Yokel RA, Florence RL, Unrine JM, Tseng MT, Graham UM, Wu P, et al. Biodistribution and oxidative stress effects of a systemically-introduced commercial ceria engineered nanomaterial. *Nanotoxicology* 2009b;3(4):234–48.
- Younce CW, Wang K, Kolattukudy PE. Hyperglycaemia-induced cardiomyocyte death is mediated via MCP-1 production and induction of a novel zinc-finger protein MCP1P. *Cardiovasc Res* 2010;87(4):665–74.
- Zhou X, Wong LL, Karakoti AS, Seal S, McGinnis JF. Nanoceria inhibit the development and promote the regression of pathologic retinal neovascularization in the vldlr knockout mouse. *PLoS One* 2011;6(2):e16733.